Beyond Rayleigh's criterion: A resolution measure with application to single-molecule microscopy

Sripad Ram*†, E. Sally Ward*, and Raimund J. Ober*‡§

*Center for Immunology, University of Texas Southwestern Medical Center, Dallas, TX 75390; †Joint Biomedical Engineering Graduate Program, University of Texas Arlington/University of Texas Southwestern Medical Center, Dallas, TX 75390; and ‡Department of Electrical Engineering, University of Texas at Dallas, Richardson, TX 75083

Rayleigh's criterion is extensively used in optical microscopy for determining the resolution of microscopes. This criterion imposes a resolution limit that has long been held as an impediment for studying nanoscale biological phenomenon through an optical microscope. However, it is well known that Rayleigh's criterion is based on intuitive notions. For example, Rayleigh's criterion is formulated in a deterministic setting that neglects the photon statistics of the acquired data. Hence it does not take into account the number of detected photons, which, in turn, raises concern over the use of Rayleigh's criterion in photon-counting techniques such as single-molecule microscopy. Here, we re-examine the resolution problem by adopting a stochastic framework and present a resolution measure that overcomes the limitations of Rayleigh's criterion. This resolution measure predicts that the resolution of optical microscopes is not limited and that it can be improved by increasing the number of detected photons. Experimental verification of the resolution measure is carried out by imaging single-molecule pairs with different distances of separation. The resolution measure provides a quantitative tool for designing and evaluating single-molecule experiments that probe biomolecular interactions.

Cramer-Rao lower bound | photon statistics | Fisher information matrix | fluorescence microscopy

According to Rayleigh's criterion, the resolution of an optical microscope is defined as the minimum distance between two point sources such that their presence can be distinguished in the image (1). It is widely believed that the resolution limit imposed by this criterion precludes the single-molecule study of molecular interactions at distances of <200 nm. Despite the widespread use of Rayleigh's criterion, it is well known that this criterion is based on heuristic notions (2). Formulated within a deterministic framework, Rayleigh's criterion neglects the stochastic nature of the photon-detection process and hence does not consider the total photon count in the acquired data. This formulation is not surprising, because Rayleigh's criterion was developed at a time when the unaided human eye was used as the detector. Therefore, Rayleigh's criterion is not well adapted to current microscope setups, in which highly sensitive photon-counting cameras are used. Recent single-molecule experiments have shown that Rayleigh's criterion can, in fact, be surpassed in an optical microscope setup (3–5). Thus Rayleigh's resolution limit is an inadequate performance criterion for current quantitative imaging techniques.

By adopting a stochastic framework, we propose a resolution measure that overcomes the shortcomings of Rayleigh's criterion and provides a quantitative measure of a microscope's ability to determine the distance between two point sources. Unlike Rayleigh's criterion our resolution measure predicts that the resolution of a microscope can be improved by increasing the number of photons collected from the point sources. The resolution measure is given in terms of quantities such as the expected number of detected photons, numerical aperture of the objective lens, and wavelength of the detected photons. We also investigate how the resolution measure is influenced by various experimental factors that affect the acquired data such as pixelation of the detector. Experimental results are presented by estimating distances from images of closely spaced single molecules. These results show that distances well below Rayleigh's resolution limit can be determined with an accuracy as specified by our resolution measure.

Results

Fundamental Resolution Measure (FREM). Our approach to the derivation of the resolution measure is to obtain a bound/limit to the accuracy with which the distance between two point sources can be estimated based on the acquired data (see *Materials and Methods*). Analogous to Rayleigh's criterion, we consider an optical microscope setup that images two identical, self-luminous, in-focus point sources emitting unpolarized, incoherent light. The analytical expression of the FREM for this imaging condition is given by

$$\delta_d := \frac{1}{\sqrt{4\pi \cdot \Lambda_0 \cdot (t - t_0) \cdot \Gamma_0(d)}} \cdot \frac{\lambda}{n_a}, \quad [1]$$

where λ denotes the emission wavelength of the detected photons, n_a denotes the numerical aperture of the objective lens, Λ_0 denotes the photon detection rate (intensity) per point source, $[t_0, t]$ denotes the acquisition time interval, and $\Gamma_0(d)$ is given by

$$\Gamma_0(d) := \int_{\mathbb{R}^2} \frac{1}{\frac{J_1^2(\alpha r_{01})}{r_{01}^2} + \frac{J_1^2(\alpha r_{02})}{r_{02}^2}} \left(\left(x + \frac{d}{2} \right) \frac{J_1(\alpha r_{01}) J_2(\alpha r_{01})}{r_{01}^3} \right.$$
$$\left. - \left(x - \frac{d}{2} \right) \frac{J_1(\alpha r_{02}) J_2(\alpha r_{02})}{r_{02}^3} \right)^2 dx\,dy, \quad [2]$$

with J_n denoting the nth order Bessel function of the first kind, $\alpha = 2\pi n_a/\lambda$; $r_{01} = \sqrt{(x + d/2)^2 + y^2}$, and $r_{02} = \sqrt{(x - d/2)^2 + y^2}$. According to Rayleigh's criterion, the minimum resolvable distance between two point sources is given by $0.61 \lambda/n_a$. The FREM, on the other hand, provides a more complex expression, which, in addition to the dependence on the ratio λ/n_a, exhibits an inverse square root dependence on other factors, i.e., the expected number of detected photons $[\Lambda_0 \cdot (t - t_0)]$ and the term $\Gamma_0(d)$ given by Eq. **2**. Note that the FREM depends on the distance of separation d through the term $\Gamma_0(d)$. Moreover, the presence of the ratio λ/n_a in $\Gamma_0(d)$ through the term α (= $2\pi n_a/\lambda$) shows that the FREM exhibits a nonlinear dependence on λ/n_a.

The stochastic framework used to obtain the FREM models the photon emission (detection) process as a random process
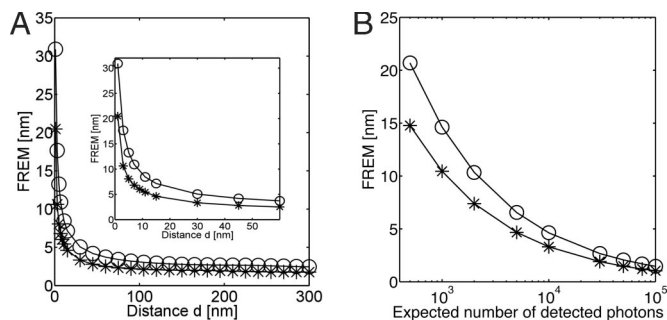

BIOPHYSICS

ENGINEERING

Fig. 1. Dependence of the FREM on distance and photon count. (*A*) The FREM as a function of the distance of separation between two point sources/single molecules. (*Inset*) The same for a distance range of 1–50 nm. (*B*) The FREM as a function of the expected number of detected photons per molecule for a distance of separation of 10 nm. In both *A* and *B*, the FREM is calculated for a pair of GFP molecules (∗) and a pair of Cy5 molecules (○). For all of the plots, the numerical aperture is set to $n_a = 1.45$ and the wavelength of the detected photons from the GFP (Cy5) molecule is set to $\lambda = 520$ nm ($\lambda = 690$ nm). In *A*, the photon detection rate Λ_0 of each GFP/Cy5 molecule is set to $\Lambda_0 = 3,000$ photons per s, and the acquisition time is set to 1 s.

(shot noise process). The spatial locations at which the photons hit the detector are assumed to be randomly distributed according to the image profiles of the point sources/single molecules. This framework considers an optical microscope setup in which the detector provides the time points and the spatial coordinates of every detected photon without adding any extraneous noise. For any imaging condition, this setup can be thought of as an idealization of current imaging detectors in which the presence of finite-sized pixels and measurement noise deteriorates the acquired data. Thus the resolution measure derived within this framework provides a result that is fundamental for the given imaging condition. In the present context, the FREM is obtained for imaging conditions analogous to those of Rayleigh's criterion. Hence the spatial distribution of the detected photons from each point source is described by the Airy profile (1).

The FREM predicts how accurately the distance d between two point sources can be resolved. A small numerical value for the FREM predicts a high accuracy in determining d, whereas a large numerical value of the FREM predicts a low accuracy in determining d. Fig. 1*A* shows the behavior of the FREM as a function of the distance of separation between a pair of GFP molecules ($\lambda = 520$ nm) and for a pair of Cy5 molecules ($\lambda = 690$ nm) that are imaged with an objective lens of numerical aperture 1.45. In Fig. 1*A*, it is assumed that the expected photon count is the same for both fluorophores. For the GFP molecules, Rayleigh's criterion predicts the smallest resolvable distance to be ≈220 nm (≈0.61 λ/n_a). In contrast, Fig. 1*A* shows that the FREM has a small numerical value for distances ranging from 50 to 220 nm, which are well below Rayleigh's criterion. For distances <50 nm, however, the FREM deteriorates (i.e., increases) significantly with decreasing distance of separation (see Fig. 1*A Inset*). In particular, as the distance of separation decreases to zero, the FREM becomes infinitely large, because the term $\Gamma_0(d)$ (Eq. **2**), which appears in the denominator of the FREM, tends to zero. An analogous behavior of the FREM is also seen for the Cy5 molecules. Note that the numerical value of the FREM for the Cy5 molecules is consistently larger than that of the GFP molecules for the same expected photon count per fluorophore. For example, the FREM predicts that a distance of 10 nm between two GFP molecules can be determined with an accuracy not better than ±5.7 nm when the expected photon count per GFP molecule is 3,000. On the other hand, for the same distance of separation and photon count per molecule, the FREM predicts an accuracy not better than ±9.1 nm for the Cy5 molecules. In the case of the Cy5 molecules, however, the numerical

value of the FREM is comparable to the distance of separation itself. Because the FREM exhibits an inverse square root dependence on the expected number of detected photons, this deterioration can be compensated for by increasing the expected number of detected photons, as shown in Fig. 1*B*. Thus in the above example, if we increase the expected photon count per Cy5 dye molecule to 10^4, then the FREM predicts that a distance of 10 nm can be determined with an accuracy not better than ±5 nm.

Practical Resolution Measure (PREM). The FREM provides the best-case scenario for a microscope setup, where experimental factors that potentially deteriorate the acquired data were not taken into account. We next investigate how the resolution measure is affected by such experimental factors. Here we obtain an analytical expression for the resolution measure that takes into account these experimental factors. We refer to this result as the PREM. The PREM can be thought of as an extension to the FREM. For instance, the PREM takes into account the presence of additive noise sources, namely Poisson and Gaussian noise. Poisson noise is used to model spurious photons in the acquired image, which, for example, arise because of the autofluorescence of the sample and dark current of the detector (6). Gaussian noise is used to model measurement noise in the acquired data, which, for example, arise during the readout process in the detector (6). The additive Poisson noise considered here is distinct from the shot noise, which describes the statistics of the photon-detection process from the single molecules and is already accounted for by the FREM. Aside from these extraneous noise sources, the PREM also takes into account the effect of pixelation of the detector.

Fig. 2*A* shows the behavior of the PREM as a function of the distance between two Cy5 molecules in the presence and absence of noise sources for a pixelated detector. Fig. 2*A* also shows the FREM for reference. Note that even in the absence of extraneous noise sources the numerical value of the PREM is consistently greater than that of the FREM because of the pixelation of the detector. Moreover, in the presence of noise sources this behavior of the PREM becomes more pronounced. In particular, for very small distances (≤50 nm), the numerical value of the PREM is at least three to five times greater than that of the FREM (see Fig. 2*A Inset*). Analogous to Fig. 1*B*, the deterioration of the PREM at very small distances can be compensated for by collecting more photons from the point sources (Fig. 2*B*). In contrast, for distances ranging from 100 to 250 nm, which are below Rayleigh's criterion (≈0.61 λ/n_a ≈ 290 nm), the numerical value of the PREM approaches that of the FREM even in the presence of noise, as shown in Fig. 2*A*. As an application of these results, consider a practical scenario in which we require distances ranging from 50 to 200 nm to be resolved between two Cy5 molecules with an accuracy of at least 5 nm. From Fig. 2*B*, we know that to estimate a distance of 50 nm with an accuracy not better than 5 nm the PREM predicts the expected number of detected photons per single molecule to be at least 15,000. On the other hand, from Fig. 2*A* we see that to estimate a distance of 200 nm with similar accuracy the PREM predicts the expected number of detected photons per single molecule to be at least 2,500. Hence to resolve distances ranging from 50 to 200 nm between two Cy5 molecules with an accuracy not better than 5 nm on average at least 15,000 photons must be collected per single molecule.

Improving the Resolution Measure by Using Additional Spatial Information. It is shown in Figs. 1*B* and 2*B* that the resolution measure can be improved by increasing the number of detected photons from each of the point sources. In single-molecule experiments increasing the photon count is not always possible, because the fluorophores may photobleach. However, for a single-molecule pair that exhibits a double-step photobleaching behavior, additional information can be obtained from the photons collected from the
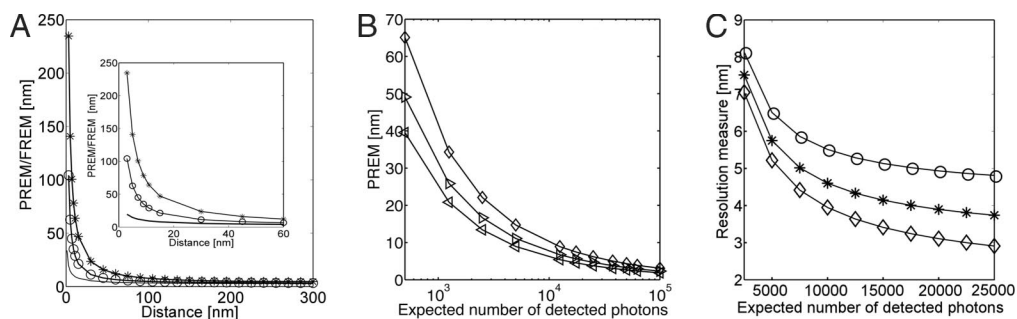
Fig. 2. Dependence of the PREM on distance and photon count. (*A*) The PREM as a function of the distance of separation between two Cy5 molecules in the presence (∗) and absence (○) of noise sources for a pixelated detector. The FREM given in Eq. **1** is also shown for reference (solid line). (*Inset*) The same for distances ranging from 1 to 60 nm. (*B*) The PREM for a pixelated detector as a function of the expected number of detected photons per molecule in the presence of noise sources for different distances of separation: $d = 30$ nm (◇), $d = 40$ nm (▷), and $d = 50$ nm (◁). (*C*) The effect of using additional spatial information on the resolution measure for a pair of Cy5 molecules ($d = 10$ nm) that exhibits a double-step photobleaching behavior. The resolution measure is shown as a function of the expected photon count collected from the single molecule after the first photobleaching event for a pixelated detector in the presence of noise sources. The plots shown consider three scenarios, i.e., when the expected number of photons collected from each single molecule before the first photobleaching event are 2,500 (○), 5,000 (∗), and 12,500 (◇). For all of the above plots, the photon detection rate Λ_0 of each Cy5 molecule is set to $\Lambda_0 = 2,500$ photons per s, the acquisition time is set to 1 s, the pixel dimension is set to 12.9×12.9 μm, the pixel array size is set to 13×13, the mean of the additive Poisson noise is set to 80 photons per pixel per s, the mean and standard deviation of the additive Gaussian noise is set to 0 e$^-$ per pixel and 8 e$^-$ per pixel, respectively, the noise statistics are assumed to be the same for all pixels, and one of the single molecules is assumed to be at the center of the pixel array. All other numerical parameters are analogous to those used in Fig. 1.

fluorophore that remains after the first photobleaching event (3). Fig. 2*C* shows the behavior of the resolution measure for a pair of Cy5 molecules spaced 10 nm apart by taking into account the number of photons collected before and after the first photobleaching event. Here the resolution measure is determined for an imaging condition with numerical values analogous to those used in Fig. 2*A*. From Fig. 2*A* we see that the resolution measure predicts an accuracy not smaller than ±5.8 nm to determine a distance of 10 nm, when on average 5,000 photons are collected from each fluorophore before and after the first photobleaching event. This result is in contrast to the case when the additional information obtained after the first photobleaching event is not used. In this case, the resolution measure predicts an accuracy not smaller than ±43.0 nm to resolve a distance of 10 nm for the same photon count per fluorophore.

Experimental Verification. The resolution measure provides a bound/limit to the smallest possible standard deviation of any unbiased estimator of the distance between the point sources. To verify whether this bound can be attained in experiments, images of closely spaced Cy5 molecules were collected, and their distances of separation were estimated by using the maximum-likelihood esti-

mator. According to Rayleigh's criterion, the minimum resolvable distance is given by $0.61 \lambda/n_a$, which, in the present case is ≈290 nm. Table 1 lists the results of distance estimation and the predicted resolution measure for two pairs of single molecules. One of the single-molecule pairs has a mean distance of separation of 293 nm (data analysis 1), which is close to Rayleigh's criterion, and the other single-molecule pair has a mean distance of separation of 207 nm (data analysis 2), which is below Rayleigh's criterion. From Table 1 we see that for each data analysis the standard deviation of the maximum-likelihood estimates of the distance comes close to the resolution measure. Note that the numerical values of the standard deviations are themselves only estimates based on the acquired data. With larger data sets, the agreement with the resolution measure is expected to increase further.

The above data sets were also analyzed by estimating the distances of separation through the global maximum-likelihood estimator (Fig. 3, which is published as supporting information on the PNAS web site), which used the additional spatial information available in the acquired data, i.e., the images collected after the first photobleaching event. Table 1 lists the results of the distance estimates (data analyses 3 and 4) for the Cy5 single-molecule pairs analyzed above. From Table 1 we see

Table 1. The mean and the standard deviation of the distance estimates calculated from experimental data and the resolution measure for each data analysis

Data analysis	Data set no.	Exposure time, s	Estimation method	N_1	N_2	Mean value of d, nm	Standard deviation of d, nm	Resolution measure for a pixelated detector, nm
1	1	3	Direct	1	0	293.2	3.6	2.8
2	2	1	Direct	1	0	206.9	10.1	7.0
3	1	3	Global	3	3	292.6	1.9	1.4
4	2	1	Global	2	2	211.6	3.8	4.4
5	3	1	Global	6	6	12.5	5.2	6.9
6	4	1	Global	4	4	14.8	8.8	7.4

Data sets 1 and 2 correspond to two closely spaced Cy5 molecules, and data sets 3 and 4 correspond to the DNA molecular ruler. The experimental data used for estimating the distances consists of time-lapse images of single-molecule pairs that exhibit a double-step photobleaching behavior. In the direct estimation method each distance estimate is obtained from an image that is acquired before the first photobleaching event. In the global estimation method, each distance estimate is obtained from two summed images. One of the summed images is obtained by adding N_1 frames that are acquired before the first photobleaching event, and the other summed image is obtained by adding N_2 frames that are acquired after the first photobleaching event. The data sets used in analyses 1 and 3 (2 and 4) are the same. For each data analysis, the resolution measure is calculated for a pixelated detector in the presence of noise sources.

that the accuracy of the distance estimates obtained by using the additional spatial information is consistently smaller than the accuracy obtained when the additional information is not used (data analyses 1 and 2). Table 1 also shows an analogous behavior of the resolution measure for the corresponding data sets. For example, in the case when the additional spatial information is not used, the standard deviation of the distance estimates for the Cy5 single-molecule pair with a mean distance of separation of 207 nm is equal to ± 10.1 nm (data analysis 2). On the other hand, for the same single-molecule pair, when additional spatial information is used the standard deviation of the distance estimates is equal to ± 3.8 nm (data analysis 4). Table 1 also lists the mean end-to-end distance estimates of the DNA molecular ruler, which were determined by using the global estimation approach (see Fig. 4, which is published as supporting information on the PNAS web site). From Table 1 it can be seen that for each DNA data set the standard deviation of the global maximum-likelihood estimator comes close to the resolution measure. For example, in data analysis 6 the standard deviation of the distance estimates is equal to ± 8.7 nm and the resolution measure predicts an accuracy not smaller than ± 7.4 nm to resolve the distance of 12 nm. We note that in the same data set, if the additional spatial information is not used, then the resolution measure predicts an accuracy not smaller than ± 52.1 nm to resolve a distance of 12 nm.

Generalization of the FREM. The FREM given in Eq. **1** was derived for imaging conditions analogous to those of Rayleigh's criterion, which considered two equal intensity, in-focus point sources that emit unpolarized, incoherent light. However, in several applications these conditions are not met, for example, when using polarized illumination and detection (7). We now consider a situation where the point sources can potentially have unequal intensities that vary as a function of time, and where the image profiles of the point sources can be distinct. The expression for the generalized FREM (g-FREM) is given by

$$\left[\frac{1}{4} \int_{t_0}^{t} \int_{\mathbb{R}^2} \frac{1}{\Lambda_1(\tau)q_1\left(x+\dfrac{d}{2},y\right) + \Lambda_2(\tau)q_2\left(x-\dfrac{d}{2},y\right)} \right. $$
$$\left. \cdot \left(\Lambda_1(\tau)\frac{\partial q_1\left(x+\dfrac{d}{2},y\right)}{\partial x} - \Lambda_2(\tau)\frac{\partial q_2\left(x-\dfrac{d}{2},y\right)}{\partial x} \right)^2 dxdyd\tau \right]^{-\frac{1}{2}},$$

[3]

where q_1 and q_2 denote the image functions of the point sources and Λ_1 and Λ_2 denote the intensities of the point sources. In many situations the image of the point source significantly differs from the Airy profile, for example, because of the defocus in the objective lens (8), the different orientations of the point-source emission dipole (7, 9), or the aberrations present in the imaging setup (10). Moreover, depending on the nature of illumination, the intensity of the point sources can be unequal when their emission dipole orientations are different (7, 9). We note that Eq. **3** provides a general expression for the FREM that is applicable to a wide variety of imaging conditions, including the above-mentioned scenarios. If in Eq. **3** we set the intensities to be constant and identical, i.e., $\Lambda_1(\tau) = \Lambda_2(\tau) = \Lambda_0$, $\tau \geq t_0$, and assume the image functions to be given by the Airy profile, then we immediately obtain the expression for the FREM given in Eq. **1**. Analogous to the g-FREM, an expression has also been derived for the generalized PREM (*see Materials and Methods*).

The stochastic framework used to derive the g-FREM models the photon detection process for each point source as a Poisson process (shot noise process). Recently, there have been reports of the generation of nonclassical states of light from a fluorescent light source in which the photon statistics deviate from the classical shot noise process (11–13). To take into account this deviation, a further generalization of the FREM can be obtained by modeling the photon detection process as a general counting process (ref. 14 and *Supporting Text*, which is published as supporting information on the PNAS web site).

Discussion

The advent of single-molecule microscopy has generated significant interest in studying nanoscale biomolecular interactions. Classically, fluorescence resonance energy transfer-based methods have been used to probe interactions in the distance range of 1 to 10 nm (15). It is widely believed that Rayleigh's criterion precludes the resolution of two single molecules at distances of <200 nm, which leaves a gap in the distance range of 10 to 200 nm that is vital for the study of many biological processes with an optical microscope. It has been suggested that Rayleigh's resolution limit can be superseded if the distance between two point sources is determined by curve fitting the image with the sum of two point-source image profiles (16). In fact, by adopting this approach several groups have shown that Rayleigh's limit can be surpassed in experiments (3–5).

The FREM (Eq. **1**) is a resolution measure that overcomes several deficiencies of Rayleigh's criterion. It gives a bound for the accuracy with which the distance between two point sources can be estimated when the acquired data are not affected by deteriorating experimental factors. An important property of the FREM is that it provides a quantitative assessment of how the optical characteristics of the experimental setup and the photon budget influence the resolution performance in determining a particular distance of separation. Fig. 1*A* shows that the numerical value of the FREM for a pair of GFP molecules is consistently smaller than that for a pair of Cy5 molecules when the expected photon count per fluorophore is 3,000 in both cases. For example, to resolve distances of 8, 50, and 200 nm between a pair of GFP molecules, the FREM predicts an accuracy not smaller than ± 6.4, ± 2.7, and ± 1.9 nm, respectively. On the other hand, for a pair of Cy5 molecules with the same expected photon count per fluorophore and distances, the FREM predicts an accuracy not smaller than ± 10.1, ± 4.0, and ± 2.7 nm, respectively. For the 50- and 200-nm distances, the numerical values of the FREM for the GFP and Cy5 molecules are significantly smaller than the corresponding actual distances. This observation implies that the FREM predicts a relatively high accuracy in resolving distances ranging from 50 to 200 nm between single molecules. For the 8-nm distance, however, the numerical value of the FREM for the GFP and Cy5 molecules are either comparable to or greater than the actual distance, which suggests that even in the best-case scenario, i.e., in the absence of deteriorating experimental factors, distances of <8 nm are difficult to resolve between the GFP/Cy5 molecules, unless a higher than average number of photons is detected. In single-molecule experiments typically 3,000 photons can be collected before a GFP molecule irreversibly photobleaches (see e.g., refs. 17 and 18), whereas for Cy5 molecules typically >10^4 photons can be collected (see ref. 19). Thus, to resolve distances of 8, 50, and 200 nm with an expected photon count of 10^4 per Cy5 molecule, the FREM predicts an accuracy not smaller than ± 5.5, ± 2.2, and ± 1.5 nm, respectively, i.e., a $\approx$2-fold improvement from the case when on average 3,000 photons are collected per Cy5 molecule. Note that the localization accuracy of a single molecule, i.e., the accuracy with which the position of a single molecule can be determined also depends on the number of collected photons (20, 21).

The PREM derived here extends the results of the FREM by illustrating how the resolution measure is deteriorated by experimental factors such as pixelation of the detector and extraneous noise sources. The PREM, i.e., the bound on the accuracy with which the distance can be estimated, for typical imaging conditions (see Fig. 2A) is given by ±31.6, ±5.3, and ±2.2 nm for the case when the Cy5 single molecules are 8, 50, and 200 nm apart, respectively, and the expected photon count per fluorophore is 10^4. For the same distances, if the expected photon count is 3,000 per Cy5 molecule, the PREM is significantly higher at ±76.7, ±12.5, and ±4.5 nm, respectively. Similarly, for a pair of GFP molecules with an expected photon count of 3,000 per molecule, the PREM predicts an accuracy not smaller than ±42.0, ±7.4, and ±3.0 nm to resolve distances of 8, 50, and 200 nm, respectively. This calculation shows that especially for small distances the predicted resolution measure is probably not acceptable for many applications. This deterioration in the limit of the accuracy with which the distance can be measured is because the acquired data are a discretized version of the actual image, and the presence of extraneous noise sources corrupts the acquired data (e.g., scattered photons, noise in the acquisition electronics). Moreover, a comparison with the FREM illustrates that control of the noise sources is also of great importance to improve the accuracy of the estimated distance parameter in a practical scenario (Fig. 2A).

The above results suggest that the distance between two single molecules can be estimated with a reasonable level of accuracy, depending on the photon count, certainly for distances >50 nm, but possibly also for smaller distances. For distances ≈10 nm, however, the predicted resolution measures are typically worse. To be able to resolve such distances the number of detected photons would have to be increased substantially, which is typically not possible because of photobleaching. For instance, if a PREM of 7 nm is to be achieved for a Cy5 single-molecule pair spaced 10 nm apart, then under the noisy imaging conditions of Fig. 2A at least 1.5×10^5 photons need to be detected per Cy5 molecule, which underscores the importance of the development of brighter and more photostable fluorescent markers to carry out such studies (7, 22).

In ref. 23 it was shown that GFP single-molecule pairs typically photobleach together. However, in the case where two-step photobleaching occurs, additional information can be used by imaging the remaining single molecule (3). The development of the FREM and the PREM discussed so far was based on the case when both point sources/single molecules do not bleach during the acquisition of the image. The approach can, however, also be applied to investigate the accuracy that can be achieved when additional information is taken into account from the remaining single molecule that did not bleach in the first photobleaching step. For example, consider a pair of GFP molecules that are 8, 15, 25, or 50 nm apart. Assume that 2,000 photons are collected from the single molecules before and after the first photobleaching event. If the photons collected before and after the first photobleaching event are taken into account, and assuming the experimental conditions for pixelation and noise sources of Fig. 2A, then an accuracy of no better than ±8.1, ±7.9, ±7.6, and ±6.7 nm, respectively, can be expected for these distances. Under the present assumptions on the expected number of detected photons, this calculation shows that for distances up to 15 nm probably unreasonably large errors would be incurred in the estimation. However, for distances >25 nm an error level of <30% could be expected.

The resolution measure provides a bound to the accuracy/standard deviation with which the distance between two point sources can be estimated. This was experimentally verified by imaging closely spaced Cy5 molecules and estimating their distance of separation from the acquired data. Here, the maximum-likelihood estimator was used, because it possesses favorable properties for estimating parameters (24). In general, other

estimation algorithms can also be used for determining the distance of separation between two point sources. However, a question that arises is which of the different estimation algorithms is the most suitable for estimating the distance of separation. In such a scenario, the knowledge of the resolution measure becomes crucial, because it can be used as a standard to compare the performance of the different estimation algorithms. The experimental results presented in Table 1 show that the standard deviations of the maximum-likelihood distance estimates come close to the bound predicted by the resolution measure, thereby validating the choice of this estimator.

The FREM was derived for imaging conditions that were analogous to those assumed in Rayleigh's criterion. In some single-molecule experiments, however, the conditions are different to those assumed in the derivation of Rayleigh's criterion and which formed the basis for the derivation of the FREM. Whereas the FREM assumes that the image of a point source is given by an Airy profile, the g-FREM was derived so that more complex image profiles can be analyzed. Such profiles could arise, for example, because of out-of-focus conditions (8), the presence of aberrations (10), or the use of polarized illumination (7). We note that the g-FREM can also be used to calculate the resolution measure for determining the distance of separation between any two (distinct) objects such as cellular organelles, provided the intensities and the image functions of the objects are known. The resolution limit of Rayleigh's criterion is thought to arise because of the finite width of the central peak of the point-source image, i.e., the point spread function (2). This approach led to the development of microscopy techniques such as 4Pi confocal microscopy (25), stimulated emission depletion microscopy (26), and image interference microscopy (27) in which the width of the central peak of the point spread function is smaller than that of the conventional optical microscope. These techniques have reported improvement in resolving features that are typically unresolvable in conventional optical microscopes. However, for some of the techniques it was reported that this improvement was achieved at a severe cost to the signal (i.e., number of collected photons) (28). This observation illustrates the importance of considering the photon/light budget when discussing resolution performance, especially in fluorescence imaging applications that typically use photobleachable fluorophores. In the present context, the expression for the FREM/g-FREM explicitly shows the tradeoff between the intensities of the point sources, which determine the photon budget, and the image functions of the point sources, which determine the point spread function shape.

Materials and Methods

Single-Molecule Microscopy. A molecular ruler consisting of a 30-bp DNA duplex was used. The oligonucleotide 5′-ATC TCG GTG CGT AAT ACT CAC GGG CAG GAC-3′ (ref. 29 and D. Holowka, personal communication) and its complementary sequence (both labeled with Cy5 at the 5′ end) were purchased from Synthegen (Houston). The oligonucleotides were annealed in 200 mM Tris·HCl, 10 mM $MgCl_2$, pH 8.0 and stored at 4°C. Molecular modeling by the vendor of the DNA duplex labeled with Cy5 dye at both ends predicts the distance between the two Cy5 dyes to be 12 nm. Cy5 dye purchased from GE Healthcare (Piscataway, NJ) was used for calibration purposes. To image single DNA molecules, a cleaned glass-bottomed dish (MatTek, Ashland, MA) was coated with a layer of polylysine (0.01% solution) followed by the fluorescent sample at a concentration of 1 pM. Imaging experiments were carried out in a custom setup that was built on a Zeiss Axiovert S100 fluorescence microscope. The setup consisted of a 643-nm laser (Research Electro-Optics, Boulder, CO), a cooled charge-coupled device camera (ORCA-ER, Hamamatsu, Bridgewater, NJ), and an αPlan-FLUAR (numerical aperture 1.45, ×100) Zeiss objective lens. The sample

was illuminated with circularly polarized light in wide-field mode, the camera was operated in 2×2 binning mode, and the exposure time was either 1 or 3 s.

Theory. Let q_1, q_2 be the image functions of the two point sources, i.e., their images at the origin of the coordinate system assuming unit magnification and normalization $\int_{\mathbb{R}^2} q_i(x, y)dxdy = 1$, $i = 1, 2$. Let $\Lambda_1(\tau)$, $\Lambda_2(\tau)$, $\tau \geq t_0$, be the intensities of the Poisson processes that model the time points of the detected photons. If the two single molecules are located a distance d apart, the impact locations of the photons on the detector plane are randomly distributed with density

$$f_{\theta,\tau}(x, y) = \frac{1}{M^2(\Lambda_1(\tau) + \Lambda_2(\tau))} \left(\Lambda_1(\tau)q_1\left(\frac{x}{M} - \frac{d}{2}, \frac{y}{M}\right) \right.$$
$$\left. + \Lambda_2(\tau)q_2\left(\frac{x}{M} + \frac{d}{2}, \frac{y}{M}\right) \right), (x, y) \in \mathbb{R}^2, \tau \geq t_0,$$

where M is the magnification and the parameter to be estimated is $\theta = d$. For this data model the Fisher information matrix is given by (14, 30)

$$\mathbf{I}(\theta) = \int_{t_0}^{t} \int_{\mathbb{R}^2} (1/\kappa_\theta(r, t))$$
$$\cdot (\partial \kappa_\theta(r, t)/\partial \theta)^T (\partial \kappa_\theta(r, t)/\partial \theta) dr d\tau,$$

where $\kappa_\theta(r, t) = (\Lambda_1(\tau) + \Lambda_2(\tau))f_{\theta,\tau}(r)$, $r \in \mathbb{R}^2$, $\tau \geq t_0$. According to the Cramer-Rao lower bound (14, 24), for the standard deviation of any unbiased estimator $\hat{\theta}$ of θ we have $\sqrt{Var(\hat{\theta})} \geq \sqrt{\mathbf{I}^{-1}(\theta)}$. We define the g-FREM as the bound on the right side of the inequality.

The data model that describes the image acquisition with a pixelated detector with N_p pixels during the integration time interval $[t_0, t]$ is given by independent random variables $\mathcal{I}_{\theta,k} = S_{\theta,k} + B_k + W_k$, where $S_{\theta,k}$ (B_k) is a Poisson random variable with mean $\mu\theta(k, t)$ ($\beta(k, t)$) that models the detected photon count at the kth pixel from the point sources (spurious sources), and W_k is an independent Gaussian random variable with mean η_k and variance $\sigma_{w,k}^2$ that models the readout noise at the kth pixel, $k = 1, \ldots, N_p$. The general expression for the Fisher information matrix $\mathbf{I}(\theta)$ is given by (21, 30)

$$\mathbf{I}(\theta) := \sum_{k=1}^{N_p} (\partial \mu_\theta(k, t)/\partial \theta)^T (\partial \mu_\theta(k, t)/\partial \theta)(\Psi_\theta(k) - 1),$$

where

$\Psi_\theta(k)$

$$:= \int_{\mathbb{R}} \frac{\left(\sum_{l=1}^{\infty} \frac{[\nu_\theta(k, t)]^{l-1} e^{-\nu_\theta(k, t)}}{(l-1)!} \cdot \frac{1}{\sqrt{2\pi}\sigma_{w,k}} e^{-\frac{1}{2}\left(\frac{z-l-\eta_k}{\sigma_{w,k}}\right)^2} \right)^2}{\frac{1}{\sqrt{2\pi}\sigma_{w,k}} \sum_{l=0}^{\infty} \frac{[\nu_\theta(k, t)]^l e^{-\nu_\theta(k, t)}}{l!} e^{-\frac{1}{2}\left(\frac{z-l-\eta_k}{\sigma_{w,k}}\right)^2}} dz,$$

and $\nu_\theta(k, t) = \mu_\theta(k, t) + \beta(k, t)$, $k = 1, \ldots, N_p$, $\theta \in \Theta$.

To obtain the Fisher information matrix for the resolution problem, the general expression for $\mathbf{I}(\theta)$ is evaluated with

$$\mu_\theta(k, t) := \frac{1}{M^2} \int_{t_0}^{t} \int_{C_k} \left(\Lambda_1(\tau)q_1\left(\frac{x}{M} - x_0, \frac{y}{M} - y_0\right) \right.$$
$$\left. + \Lambda_2(\tau)q_2\left(\frac{x}{M} - x_0 - d\cos\phi, \frac{y}{M} - y_0 - d\sin\phi\right) \right)$$
$$dxdy, k = 1, \ldots, N_p,$$

where C_k denotes the kth pixel, (x_0, y_0) denotes the location of one of the point sources, ϕ denotes the angle subtended by the line joining the two point sources, and $\theta = (x_0, y_0, d, \phi)$ (Fig. 5, which is published as supporting information on the PNAS web site).

According to the Cramer-Rao lower bound, the bound on the standard deviation of any unbiased estimator of the distance d is $\sqrt{[\mathbf{I}^{-1}(\theta)]_{33}}$, where $[\mathbf{I}^{-1}(\theta)]_{33}$ denotes the third leading-diagonal entry of $\mathbf{I}^{-1}(\theta)$, i.e., the entry that corresponds to the distance parameter. We refer to this bound as the generalized PREM.

Evaluating the g-FREM (generalized PREM) for the special case of identical photon detection rates $\Lambda_1(\tau) = \Lambda_2(\tau) = \Lambda_0$, $\tau \geq t_0$, and assuming that q_1, q_2 are given by the Airy profile, we obtain the FREM (PREM). See *Supporting Text* for more details and discussion.

Data Analysis. The single-molecule images were analyzed and processed by using MATLAB (Mathworks, Natick, MA). The single-molecule pairs were identified by their double-step photobleaching behavior. Before estimating the unknown parameters, the expected number of detected photons of the single molecules, the background photon count, and the parameter α were first independently determined from the single-molecule images. The parameters were then estimated by the method of maximum likelihood (see *Supporting Text*).

1. Born, M. & Wolf, E. (1999) *Principles of Optics* (Cambridge Univ. Press, Cambridge, U.K.).
2. Inoue, S. & Spring, K. R. (1997) *Video Microscopy: The Fundamentals* (Plenum, New York).
3. Gordon, M. P., Ha, T. & Selvin, P. R. (2004) *Proc. Natl. Acad. Sci. USA* **101,** 6462–6465.
4. Qu, X., Wu, D., Mets, L. & Scherer, N. F. (2004) *Proc. Natl. Acad. Sci. USA* **101,** 11298–11303.
5. Lidke, K. A., Rieger, B., Jovin, T. M. & Heintzmann, R. (2005) *Opt. Exp.* **13,** 7052–7062.
6. Snyder, D. L., Helstrom, C. W., Lanterman, A. D., Faisal, M. & White, R. L. (1995) *J. Opt. Soc. Am. A* **12,** 272–283.
7. Moerner, W. E. & Fromm, D. P. (2003) *Rev. Sci. Instrum.* **74,** 3597–3619.
8. Sheppard, C. J. R. & Török, P. (1997) *Bioimaging* **5,** 205–218.
9. Enderlein, J. (2000) *Opt. Lett.* **25,** 634–636.
10. Török, P., Varga, P., Laczik, Z. & Booker, G. R. (1995) *J. Opt. Soc. Am. A* **12,** 2660–2671.
11. Lounis, B. & Moerner, W. E. (2000) *Nature* **407,** 491–493.
12. Fleury, L., Segura, J. M., Zumofen, G., Hecht, B. & Wild, U. (2000) *Phys. Rev. Lett.* **84,** 1148–1151.
13. Tinnefeld, P., Müller, C. & Sauer, M. (2001) *Chem. Phys. Lett.* **345,** 252–258.
14. Snyder, D. L. & Miller, M. I. (1991) *Random Point Processes in Time and Space* (Springer, Berlin).
15. Roessel, P. V. & Brand, A. H. (2002) *Nat. Cell Biol.* **4,** E15–E20.
16. Hobbs, P. C. D. (2000) *Building Electro-Optical Systems* (Wiley, New York).
17. Kubitscheck, U., Kückmann, O., Kues, T. & Peters, R. (2000) *Biophys. J.* **78,** 2170–2179.
18. Mashanov, G. I., Tacon, D., Peckham, M. & Molloy, J. E. (2004) *J. Biol. Chem.* **279,** 15274–15280.
19. Tinnefeld, P., Herten, D. P. & Sauer, M. (2001) *J. Phys. Chem. A* **105,** 7989–8003.
20. Thompson, R. E., Larson, D. R. & Webb, W. W. (2002) *Biophys. J.* **82,** 2775–2783.
21. Ober, R. J., Ram, S. & Ward, E. S. (2004) *Biophys. J.* **86,** 1185–1200.
22. Alivisatos, A. P., Gu, W. & Larabell, C. (2005) *Annu. Rev. Biomed. Eng.* **7,** 55–76.
23. Balci, H., Ha, T., Sweeney, H. L. & Selvin, P. R. (2005) *Biophys. J.* **89,** 413–417.
24. Zacks, S. (1971) *The Theory of Statistical Inference* (Wiley, New York).
25. Hell, S. & Stelzer, E. H. K. (1992) *J. Opt. Soc. Am. A* **9,** 2156–2166.
26. Klar, T. A., Jakobs, S., Dyba, M., Egner, A. & Hell, S. W. (2000) *Proc. Natl. Acad. Sci. USA* **97,** 8206–8210.
27. Gustafsson, M., Agard, D. A. & Sedat, J. W. (1999) *J. Microsc. (Oxford)* **195,** 10–16.
28. Gustafsson, M. (1999) *Curr. Opin. Struct. Biol.* **9,** 627–634.
29. Paar, J. M., Harris, N. T., Holowka, D. & Baird, B. (2002) *J. Immunol.* **169,** 856–864.
30. Ram, S., Ward, E. S. & Ober, R. J. (2006) *Multidim. Sys. Sig. Proc.* **17,** 27–58.